UAV-BASED GLACIER MONITORING: GNSS KINEMATIC TRACK POST-PROCESSING AND DIRECT GEOREFERENCING FOR ACCURATE RECONSTRUCTIONS IN CHALLENGING

UAV-BASED GLACIER MONITORING: GNSS KINEMATIC TRACK POST-PROCESSING AND DIRECT GEOREFERENCING FOR ACCURATE RECONSTRUCTIONS IN CHALLENGING ENVIRONMENTS

V. Belloni[1,*], D. Fugazza[2], M. Di Rita[3]

[1] Geodesy and Geomatics Division, DICEA, Sapienza University of Rome, Rome, Italy - valeria.belloni@uniroma1.it
[2] Department of Environmental Science and Policy, University of Milan, Milan, Italy - davide.fugazza@unimi.it
[3] Leica Geosystems AG, Heerbrugg, Switzerland - martina.di-rita@leica-geosystems.com

Commission I, ICWG I/II

KEY WORDS: UAV photogrammetry, UAV GNSS track post-processing, Direct georeferencing, Glacier monitoring.

ABSTRACT:

Continuous monitoring of glaciers is of key importance to understand their morphological evolution over time and monitor the impact of climate change. Recently, Unmanned Aerial Vehicles (UAVs) have proven to be ideal candidates for glacier monitoring thanks to their flexibility and ease of processing with software packages. Traditionally, for high-accurate and geodetically relevant results, Ground Control Points (GCPs) need to be homogeneously distributed over the area of interest and manually identified in the imagery to guarantee accurate reconstructions. However, the GCP setup is always time consuming and, in many cases, a difficult operation due to logistic constraints. Nowadays, many UAVs offer GNSS Real Time Kinematic (RTK) capabilities that usually highly improve 3D reconstructions. However, there are circumstances in which an RTK solution cannot be directly achieved in the field. This is particularly frequent in challenging mountain environments such as glaciers. In such cases, post-processing UAV GNSS kinematic tracks could represent a powerful approach for improving the quality of 3D models. The goal of this work is to investigate the potential of UAV track post-processing combined with direct georeferencing for accurate 3D reconstructions without the need for GCPs in a complex environment of an Alpine glacier. The study area is Forni Glacier in the Rhaetian Alps, Italy. The data were acquired during two campaigns performed in August 2020 and August 2021 and include UAV images captured using a DJI Phantom 4 RTK and target positions measured with Leica GS18 I receivers. The data were processed using a pipeline entirely implemented in the Leica Infinity software that combines GNSS post-processing, a standard photogrammetric pipeline and a new tool to post-process GNSS kinematic tracks of UAVs. The approach based on UAV track post-processing and direct georeferencing was assessed using the acquired targets as Check Points (CPs) and compared to a standard photogrammetric approach in terms of glacier height loss computation. The results show Root Mean Square Errors (RMSEs) of the CPs below 4 cm for both the 2020 and 2021 campaigns. As for glacier height loss computation, the DPCs generated from the two surveys using a standard photogrammetric approach and a workflow based on UAV track post-processing and direct georeferencing were differentiated to compute the height differences of the glacier surfaces over one year. The two investigated approaches show similar results with an average height loss of 5 metres measured on the glacier tongue and demonstrate that UAV track post-processing can compensate for the RTK signal loss allowing accurate 3D reconstruction and eliminating the need for GCPs, especially if pre-calibration is performed.

1. INTRODUCTION

Glaciers play an important role by providing freshwater that can be used for domestic, industrial and agricultural applications. Changes in glaciers may, therefore, directly impact human livelihoods. Furthermore, they are strong indicators of climate change since they are highly influenced by changes in precipitation and temperature. Continuous monitoring of glaciers is therefore crucial to better understand their morphological evolution over time, forecast water availability and monitor climate change. Among the parameters adopted for glacier monitoring, mass balance is one of the most important. The mass balance can be computed from the total volume loss which is usually evaluated from the height change of a glacier body that occurs between two consecutive survey epochs (i.e. the multi-temporal difference of the glacier Dense Point Clouds - DPCs or Digital Surface Models - DSMs). However, the accurate retrieval of glacier morphology changes is not an easy task. Over the past decades, different approaches have been investigated: GNSS surveys, terrestrial laser scanning, satellite imagery and Unmanned Aerial Vehicles (UAVs) (Fugazza et al., 2018, Immerzeel et al., 2014, Scaioni et al., 2017, Scaioni et al., 2018, Tonolo et al., 2020). Compared to the other techniques, UAV campaigns enable the collection of data over wide and inaccessible areas in an efficient way. The cost involved in data acquisition is relatively low and users can easily acquire data according to their schedule (Bhardwaj et al., 2016). Moreover, the combination of UAVs with Structure-from-Motion (SfM) and dense matching techniques allows the reconstruction of the 3D point cloud and the 3D surface of the glacier with high accuracy and high efficiency (Di Rita et al., 2020). Traditionally, the combination of UAV data with the SfM technique implemented in the photogrammetric processing relies on Ground Control Points (GCPs) which need to be homogeneously distributed and measured inside the study area to link the image plane coordinates into 3D world coordinates (indirect georeferencing). It is also worth noting that GCPs can be used for fine-tuning the camera parameters especially if pre-calibration cannot be performed due to logistic constraints and limited time. How-

* Corresponding author

ever, the GCP setup requires labour-intensive, time-consuming, and potentially risky manual fieldwork which reduces the benefits of remote sensing approaches, especially in mountain areas where all the operations should be carried out as fast as possible due to the quickly changing environmental conditions (Maier et al., 2022).

Nowadays, many UAVs offer GNSS Real Time Kinematic (RTK) capabilities that usually highly improve the collection of data and the accuracy of the reconstruction. In theory, the employment of an RTK UAV may directly provide sufficient accuracy for image orientation also when GCPs are scarce or not available at all (direct georeferencing). Also, it removes the need for human interaction to identify GCPs within the imagery (Rabah et al., 2018, Taddia et al., 2020, Gabrlik et al., 2018). It is, therefore, a promising approach since it greatly facilitates data acquisition and it reduces the costs and the required expertise allowing an automatic processing chain (Turner et al., 2014). Previous studies (Dall'Asta et al., 2017) in the Alpine environment demonstrated that by combining RTK technology and direct georeferencing the RMSEs (Root Mean Square Errors) of the differences found on 12 Check Points (CPs) were about 4 cm in horizontal and 7 cm in elevation, i.e. practically the same accuracy found using GCPs. Anyway, there are circumstances in which an RTK accurate solution cannot be directly achieved in the field even using a reference station or a connection to a reference station cannot be set up. Indeed, in challenging environments such as glaciers, RTK is prone to losing either the satellite or the radio signal due to occlusions or long distances between the UAV platform and the reference drone station. Finally, the use of the RTK technology still introduces a potential error related to the reference system of the acquired camera centres. For all these reasons, post-processing of UAV GNSS tracks could represent a powerful approach to improving the quality of 3D reconstructions. When RTK is not available, the non-real-time Post Processing Kinematic (PPK) approach can be adopted to post-process the raw GNSS data of the UAV using a GNSS reference station placed near the area of interest.

The present work aims to investigate the potential of UAV GNSS kinematic track post-processing for improving the accuracy of 3D reconstructions in a complex environment and computing the glacier loss over time from multi-temporal DPC differencing, given that the camera is pre-calibrated. The impact of UAV GNSS kinematic track post-processing is investigated using a direct georeferencing approach to demonstrate that it can compensate for the loss of RTK signal and eliminate the need for GCPs. The workflow based on UAV track post-processing and direct georeferencing is assessed using the available targets as CPs and then compared to a standard photogrammetric workflow in terms of glacier height loss computation. The study area is Forni Glacier, one of the largest Italian glaciers (Paul et al., 2020), located in the Central Italian Alps, Stelvio National Park. The glacier has undergone rapid retreat and profound morphological changes in recent years and it has been monitored over time with different techniques (Azzoni et al., 2017, Fugazza et al., 2018, Scaioni et al., 2018). The complex morphology of the glacier environment, typical of mountain areas, usually introduces some challenges during data collection. Among them, the acquisition of UAV data in RTK mode presents some limitations due to the large extension of the area and possible occlusions. Also, in this type of environment, the difficulties related to the GCP setup usually lead to a sub-optimal target distribution that can highly affect the results. The area represents, therefore, a good case study to investigate the impact of UAV track post-processing combined with direct georeferencing.

2. DATA COLLECTION

The campaigns were carried out during three days of acquisition between August 20 and 22, 2020 and August 19 and 21, 2021 in the area of Forni Glacier. Different UAV surveys were performed using a DJI Phantom 4 RTK equipped with a multi-constellation multi-frequency GNSS receiver able to receive GPS, GLONASS, Galileo and Beidou signals. Furthermore, the UAV has an integrated RTK module that provides real-time, centimetre-level positioning data for improved absolute accuracy on image metadata (DJI Development Team, 2022). When used in planned flight mode, the DJI Phantom 4 RTK also stores satellite observation data to be used for PPK in case the RTK connection is lost or not available. For all these reasons, the DJI Phantom 4 RTK was considered the most suitable option for capturing the data on the glacier environment and investigating UAV track post-processing. The main technical specifications of the adopted UAV are presented in Table 1.

Weight	1391 g
Average flight time	30 minutes
Camera model	FC6310R
Sensor	1" CMOS - 20 MP
Focal length	8.8 mm
Image resolution	5472×3648 pixel

Table 1. Technical specifications of the DJI Phantom 4 RTK.

In the campaign, the DJI Phantom 4 RTK was combined with a D-RTK 2 high precision GNSS mobile station to allow the drone RTK navigation (Figure 1).

Figure 1. DJI Phantom 4 RTK and D-RTK 2 high precision GNSS mobile station.

The DJI station was placed in a fixed position outside the glacier tongue to guarantee a good connection with the UAV during all the flights. However, as expected, in a few cases the RTK connection between the UAV and the drone station was lost due to environmental conditions. Before flying the drone, the coordinates of the DJI station were measured using a Leica GS18 I receiver. Then, the UAV flights were planned and carried out by using the DJI flight remote controller which allowed the UAV to connect to the DJI station in the RTK survey mode and follow predefined waypoints to capture images with a fixed overlap. However, due to the low accuracy of the DJI drone station, the image positioning, even in RTK mode, presented a translation with respect to the target coordinates and introduced some challenges during data processing. In August 2020 and August 2021, the UAV was flown with a speed of 3.5 m/s and a flying height of approximately 100 m above the glacier surface, which resulted in an average Ground Sample Distance (GSD) of 2.6 cm/pixel. The performed UAV flights allowed the acquisition of images in JPG format with an along-track overlap between 75 % and 80 %. For all the flights, the image rate was properly set to optimise data acquisition and guarantee both redundancy and efficiency. During the fieldwork, some targets were placed over the area of interest prior to the UAV flights. Both artificial and natural targets were used to speed up data acquisition. In general, artificial plastic targets guarantee a more accurate manual collimation which is crucial for the processing but they need to be distributed over the area of interest and then removed at the end of the survey. Natural targets can be easily realised with stones and wood during the campaign and they do not need to be collected at the end of the fieldwork. However, in case natural targets are used, the results can be partially affected by errors due to sub-optimal manual collimation. The use of natural targets can be, therefore, less time consuming but also less accurate. An example of the adopted artificial and natural targets is presented in Figure 2.

Figure 2. Artificial and natural targets.

The target 3D coordinates were surveyed using a Leica GS18 I multi-frequency GNSS receiver connected in RTK survey mode with a second Leica GS18 I placed at the Branca hut (2943 m) in a static position during the survey.

3. METHODOLOGY AND DATA PROCESSING

For processing the data, the GNSS and photogrammetric pipeline implemented in the Leica Infinity software (Leica Infinity Development Team, 2022) was adopted. Leica Infinity is a geospatial surveying software focused on workflows to easily process, combine and integrate data collected from different kinds of sensors such as GNSS receivers, total stations, laser scanners and UAVs (Di Rita et al., 2020). To process UAV data, Leica Infinity adopts the SfM algorithm to reconstruct 3D surfaces starting from a set of overlapping images. Firstly, tie points are identified and matched among the acquired images. Then, a highly redundant bundle adjustment is used to solve the scene geometry and the camera pose simultaneously (Westoby et al., 2012). Finally, based on the extracted features a Sparse Point Cloud (SPC) is firstly generated and then densified through dense matching techniques to obtain a DPC and the corresponding DSM and Orthophoto. Among other things, the latest version released in November 2021 (Leica Infinity 3.6.1) also implements a tool to post-process GNSS kinematic tracks of UAVs. This tool works for Leica AX20 and DJI drones able to store raw GNSS data and is dedicated to improve image positioning accuracy and derive the best possible final deliverables, i.e. DPCs, DSMs and Orthophotos. At the moment, Leica Infinity is the best solution available in the market since it allows GNSS data post-processing, UAV GNSS kinematic track post-processing and standard photogrammetric pipeline in one software and in a common reference frame.

In the present work, the processing chain was entirely carried out in Leica Infinity. The first step of processing focused on the GNSS data measured using the Leica receivers. Firstly, the position of the Leica GS18 I placed at the Branca hut was post-processed using the GNSS reference stations of Bienno and Tirano (HxGN Smartnet network). Then, all the acquired 3D coordinates of the targets were corrected using the post-processed position of the static Leica GS18 I receiver placed at the Branca hut. During the second step, the photogrammetric pipeline of Leica Infinity was adopted. In the first place, the data from the 2020 and 2021 campaigns were processed following a standard photogrammetric workflow using pre-calibrated camera parameters and the available targets as GCPs, without post-processing the GNSS kinematic tracks of the drone. The image orientation was computed, based on SfM integrated with bundle block adjustment, to derive SPCs and DPCs. Finally, by continuing the work started in a previous study (Di Rita et al., 2020), the DPCs generated from the 2020 and 2021 campaigns were compared to evaluate the loss of Forni Glacier during one year. Specifically, the glacier height differences were computed by differencing the reconstructed DPCs using the Comparison Map tool available in Leica Infinity. The adopted flowchart is shown in Figure 3.

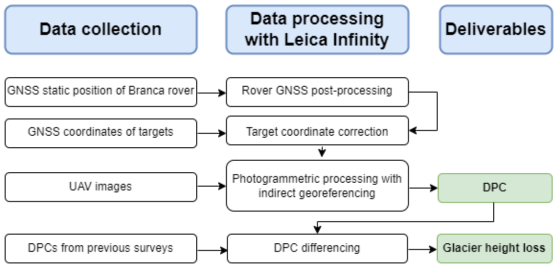

Figure 3. Processing flowchart based on a standard photogrammetric pipeline.

Then, a second independent processing was carried out on the raw data, including the UAV GNSS kinematic track post-processing as the first step, to assess its impact on the accuracy of the reconstruction. The UAV GNSS track post-processing was performed using the post-processed position of the Branca rover as reference. After UAV track post-processing, the image orientation was carried out (with pre-calibrated camera parameters) through a direct georeferencing approach and the accuracy was evaluated using the available targets as CPs. The DPCs of the two campaigns were generated as in the previous flowchart and compared to evaluate the glacier height loss. The flowchart of the described processing is shown in Figure 4.

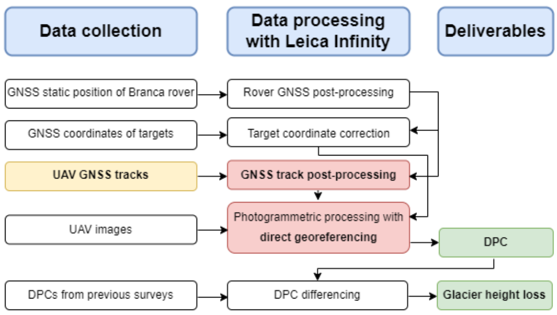

Figure 4. Processing flowchart based on UAV track post-processing and direct georeferencing.

https://doi.org/10.5194/isprs-archives-XLIII-B1-2022-367-2022

The data were processed separately for the two campaigns. In the present work, the focus is on a small area on the tongue of Forni Glacier which is highly subjected to rapid changes. The 2020 image block is composed of 298 images captured during 4 flights: 2 of them were entirely performed in RTK survey mode while during the others the RTK connection was lost. For all the flights GNSS data of the tracks were also acquired. The block of images covers an area containing 8 targets with known 3D positions. The image and target distribution of the 2020 block is shown in Figure 5.

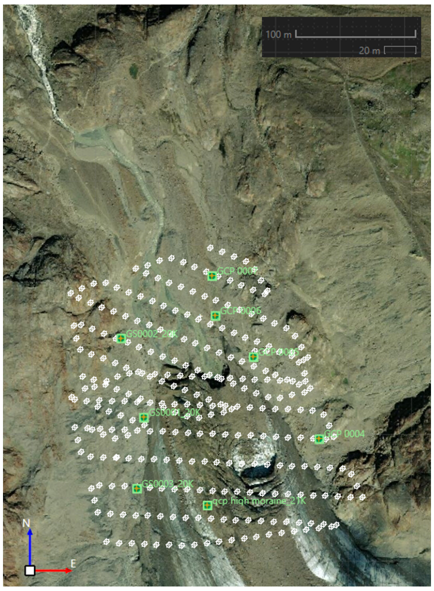

Figure 5. UAV tracks and target distribution - 2020 block.

The 2021 block is composed of 460 images (all acquired in RTK mode with store of GNSS data of the UAV tracks) and covers an area containing 12 targets with known 3D positions. Due to the sub-optimal target distribution, a wider block compared to the 2020 image group was considered in this case. The image and target distribution of the 2021 block is shown in Figure 6.

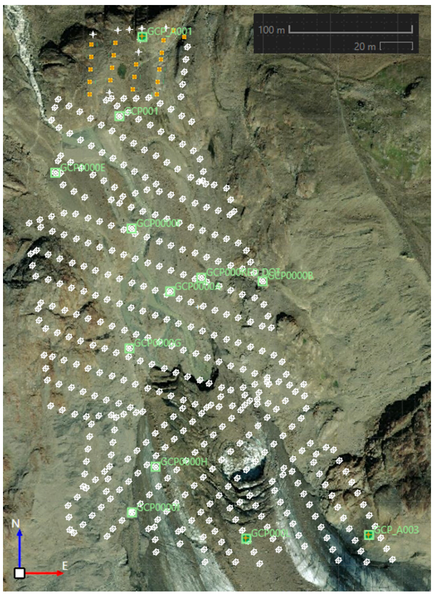

Figure 6. UAV tracks and target distribution - 2021 block.

4. RESULTS AND DISCUSSION

4.1 Result assessment

An assessment of the results achieved using the data from the two campaigns is here presented. Table 2 and Table 3 refer to the orientation of the 2020 block using the standard photogrammetric pipeline and the approach based on UAV GNSS track post-processing. Specifically, Table 2 shows the results of the orientation step using a standard photogrammetric pipeline without post-processing the GNSS tracks of the drone and using the indirect georeferencing approach based on GCPs.

GCP id	ΔE [m]	ΔN [m]	ΔH [m]	Mean Repr. Error [px]	Images Marked n.
0004	0.004	0.004	-0.012	0.5	12
0005	0.000	-0.005	-0.013	0.5	13
0006	0.003	0.010	0.015	0.5	12
0007	0.022	0.010	0.011	0.9	12
mor 21K	0.021	-0.004	0.010	1.0	10
01 20K	-0.006	0.008	0.004	0.4	10
02 20K	-0.007	-0.002	-0.006	0.4	10
03 20K	-0.001	-0.005	0.018	0.5	11
Mean	**0.004**	**0.002**	**0.003**	**0.6**	-
SD	**0.011**	**0.007**	**0.012**	**0.2**	-

Table 2. Assessment of the standard photogrammetric pipeline - 2020 block.

Residual errors in Easting, Northing and Orthometric Height are shown for each GCP together with the Mean Reprojection Error. The results highlight Standard Deviation (SD) values in Easting, Northing and Orthometric Height below 2 cm and Mean Reprojection Errors below the pixel. Table 3 shows the results of the orientation step of the 2020 block using post-processing of UAV GNSS tracks and direct georeferencing. The accuracy of the processing was evaluated using all the available targets as CPs.

CP id	ΔE [m]	ΔN [m]	ΔH [m]	Mean Repr. Error [px]	Images Marked n.
0004	-0.004	0.000	0.080	1.7	12
0005	0.009	0.001	-0.008	0.5	13
0006	0.009	0.023	-0.016	0.8	12
0007	0.034	0.023	-0.041	1.3	12
mor 21K	-0.005	-0.004	0.012	0.4	10
01 20K	-0.022	0.019	-0.015	1.0	10
02 20K	-0.018	0.002	-0.021	0.8	10
03 20K	-0.030	0.009	-0.008	1.2	11
Mean	**-0.003**	**0.009**	**-0.002**	**1.0**	-
SD	**0.021**	**0.011**	**0.036**	**0.4**	-
RMSE	**0.020**	**0.014**	**0.034**	**1.1**	-

Table 3. Assessment with UAV track post-processing and direct georeferencing - 2020 block.

The results show SD and RMSE values in Easting, Northing and Orthometric Height below 4 cm and Mean Reprojection Error of 1 pixel.

Table 4 and Table 5 refer to the processing of the data acquired during the 2021 survey. Table 4 shows the results of the orientation step without post-processing the GNSS tracks of the drone and using all the available targets as GCPs.

GCP id	ΔE [m]	ΔN [m]	ΔH [m]	Mean Repr. Error [px]	Images Marked n.
A001	-0.004	-0.007	0.046	0.4	10
A003	-0.004	0.013	0.011	1.0	6
0000A	0.002	-0.019	-0.020	0.7	9
0000B	-0.029	0.019	0.067	2.3	4
0000E	-0.008	0.011	0.038	0.5	10
0000F	0.005	-0.002	0.029	0.5	10
0000G	0.001	-0.014	-0.003	0.6	10
0000H	0.013	-0.018	-0.073	1.1	10
0000I	0.010	-0.003	0.029	0.6	10
0000L	0.013	-0.001	0.008	0.5	10
Red Dot	-0.012	0.006	-0.042	0.9	10
001	-0.012	0.000	0.028	0.4	10
Mean	**-0.002**	**-0.001**	**0.010**	**0.8**	-
SD	**0.012**	**0.012**	**0.039**	**0.5**	-

Table 4. Assessment of the standard photogrammetric pipeline - 2021 block.

The results highlight SD values in Easting, Northing and Orthometric Height below 4 cm and Mean Reprojection Error of 0.8 pixel. Finally, Table 5 shows the results of the orientation step of the 2021 block achieved by combining post-processing of the UAV GNSS kinematic tracks and direct georeferencing.

CP id	ΔE [m]	ΔN [m]	ΔH [m]	Mean Repr. Error [px]	Images Marked n.
A001	0.012	-0.040	-0.018	1.3	10
A003	0.006	0.000	0.040	1.1	6
0000A	0.001	-0.006	0.024	0.5	9
0000B	-0.013	-0.013	0.050	0.9	4
0000E	-0.018	0.019	0.069	0.8	10
0000F	0.001	0.005	0.052	0.8	10
0000G	-0.010	0.000	0.028	0.5	10
0000H	-0.002	-0.004	0.020	0.4	10
0000I	-0.003	-0.014	0.008	0.6	10
0000L	-0.005	-0.016	0.058	0.9	10
Red Dot	-0.006	0.013	0.008	0.6	10
001	-0.016	0.002	0.028	0.5	10
Mean	**-0.004**	**-0.005**	**0.031**	**0.7**	-
SD	**0.009**	**0.015**	**0.025**	**0.3**	-
RMSE	**0.010**	**0.015**	**0.039**	**0.8**	-

Table 5. Assessment with UAV track post-processing and direct georeferencing - 2021 block.

Again, the SD and RMSE values in Easting, Northing and Orthometric Height are below 4 cm and the Mean Reprojection Error is below the pixel. The results demonstrate that, if UAV track post-processing is adopted and camera calibration is performed before flying, 3D reconstructions with a sufficient accuracy for the final goal are achieved without using GCPs. It is also worth noting that all the adopted 3D points are artificial targets except for point A003 which is a natural target made of stones. The accuracy assessment highlights that the error of the natural target is comparable with the residuals achieved on the artificial 3D points, demonstrating that natural targets can be also a valuable solution to speed up data acquisition.

4.2 DPC generation

After image orientation, the 2020 and 2021 DPCs were generated in Leica Infinity using both approaches. Figures 7 and Figure 8 show the 2020 and 2021 DPCs of Forni Glacier generated with UAV track post-processing and direct georeferencing.

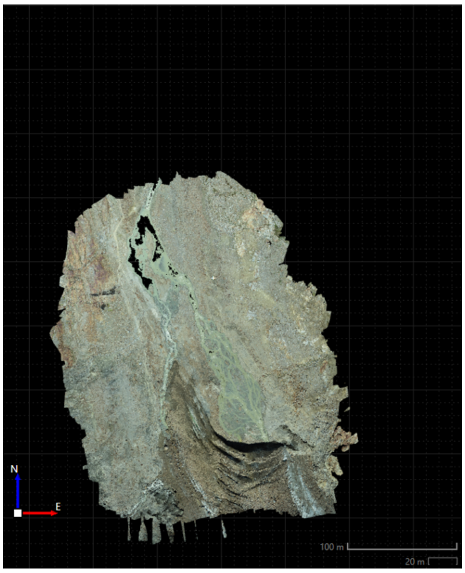

Figure 7. 2020 DPC - UAV track post-processing and direct georeferencing.

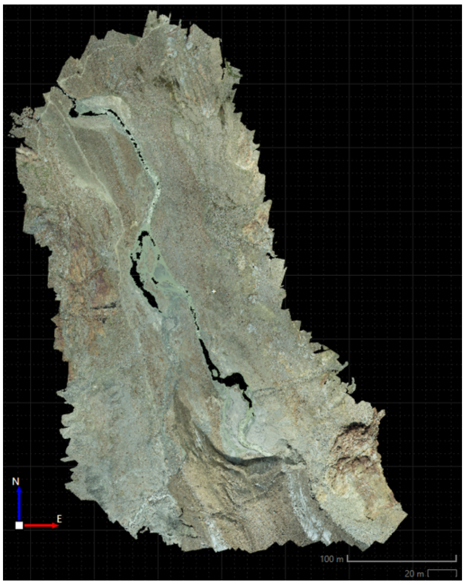

Figure 8. 2021 DPC - UAV track post-processing and direct georeferencing.

4.3 DPC differencing and glacier height loss computation

Finally, the DPC from the 2020 survey was subtracted from the DPC generated using the 2021 dataset to evaluate the evolution and changes of the glacier body. The procedure was adopted for both the indirect and direct georeferencing approaches. The corresponding height comparison maps computed in Leica Infinity are shown in Figure 9 and Figure 10.

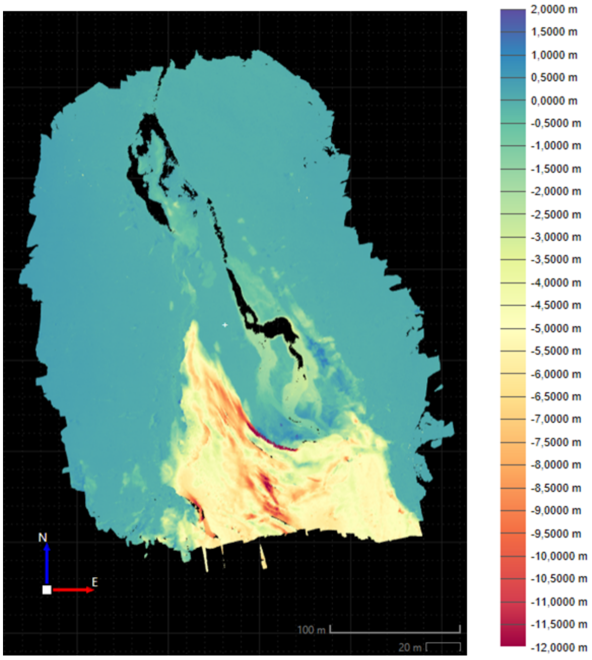

Figure 9. Height comparison map between the 2020 and 2021 DPCs - standard photogrammetric pipeline.

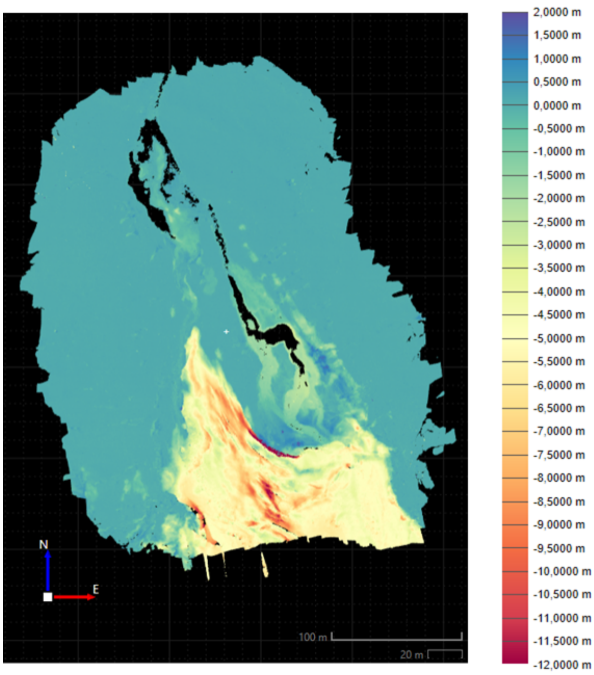

Figure 10. Height comparison map between the 2020 and 2021 DPCs - UAV track post-processing and direct georeferencing.

The comparison maps highlight similar results with an average height loss of 5 metres measured on the glacier tongue. Also, the height differences outside the area subjected to changes are close to zero, which indicates the good accuracy of the 3D reconstructions with both approaches. The comparison also demonstrates that UAV track post-processing can guarantee accurate reconstructions even without the use of GCPs.

5. CONCLUSIONS

In the present work UAV GNSS kinematic track post-processing was investigated in combination with direct georeferencing. Two campaigns were carried out in August 2020 and August 2021 in an Alpine environment. The two surveys allowed the acquisition of images and target positions captured using a DJI Phantom 4 RTK drone and GNSS GS18 I Leica receivers. The study area is Forni Glacier in Stelvio National Park (Rhaetian Alps, Italy). The data were processed with Leica Infinity using the new tool for UAV GNSS kinematic track post-processing implemented in the software. This tool allowed compensation for the loss of RTK connection during the acquisition in the challenging mountain environment and guaranteed accurate 3D reconstructions of the glacier body for loss computation even without GCPs. To assess the potential of kinematic track post-processing, different processings were performed. Firstly, the data were processed using a standard photogrammetric approach based on GCPs and pre-calibrated camera parameters. Then, a second independent processing was carried out on the raw data, including the UAV GNSS kinematic track post-processing as the first step and using a direct georeferencing approach without GCPs. Again, pre-calibrated camera parameters were used. The results of UAV track post-processing and direct georeferencing highlight RMSEs of the CPs below 4 cm, demonstrating the good performance of UAV GNSS kinematic track post-processing for 3D reconstructions. Finally, the DPCs obtained from the data acquired in 2020 and 2021 were differentiated to estimate the glacier height changes and compare the performances of the two investigated approaches. The comparison maps highlight similar results and an average height loss of 5 metres on the glacier tongue. This study showed the potential of the photogrammetric pipeline, the new UAV post-processing and the analysis tools implemented in the Leica Infinity software for 3D model generation and glacier monitoring. The work also confirmed the potential of UAV data combined with post-processing techniques for glacier morphology change assessment even when the acquisition conditions are problematic (lack of GCPs, RTK signal loss, inaccurate in-situ measurements).

ACKNOWLEDGEMENTS

The present study was partially supported by Levissima Sanpellegrino S.P.A. through an agreement with UNIMI. The authors would like to thank Leica Geosystems AG for providing the surveying instruments and Stelvio Park Authority for the logistic and financial support and for permitting the UAV surveys.

REFERENCES

Azzoni, R. S., Fugazza, D., Zennaro, M., Zucali, M., D'Agata, C., Maragno, D., Cernuschi, M., Smiraglia, C., Diolaiuti, G. A., 2017. Recent structural evolution of Forni Glacier tongue (Ortles-Cevedale Group, Central Italian Alps).

Journal of Maps, 13(2), 870-878. https://doi.org/10.1080/17445647.2017.1394227.

Bhardwaj, A., Sam, L., Akanksha, Martin-Torres, F. J., Kumar, R., 2016. UAVs as remote sensing platform in glaciology: Present applications and future prospects. *Remote Sensing of Environment*, 175, 196-204. https://www.sciencedirect.com/science/article/pii/S0034425715302509.

Dall'Asta, E., Forlani, G., Roncella, R., Santise, M., Diotri, F., Morra di Cella, U., 2017. Unmanned Aerial Systems and DSM matching for rock glacier monitoring. *ISPRS Journal of Photogrammetry and Remote Sensing*, 127, 102-114. https://www.sciencedirect.com/science/article/pii/S0924271616304233.

Di Rita, M., Fugazza, D., Belloni, V., Diolaiuti, G., Scaioni, M., Crespi, M., 2020. GLACIER VOLUME CHANGE MONITORING FROM UAV OBSERVATIONS: ISSUES AND POTENTIALS OF STATE-OF-THE-ART TECHNIQUES. *The International Archives of the Photogrammetry, Remote Sensing and Spatial Information Sciences*, XLIII-B2-2020, 1041–1048. https://www.int-arch-photogramm-remote-sens-spatial-inf-sci.net/XLIII-B2-2020/1041/2020/.

DJI Development Team, 2022. Dji phantom 4 rtk. https://www.dji.com/ie/phantom-4-rtk.

Fugazza, D., Scaioni, M., Corti, M., D'Agata, C., Azzoni, R. S., Cernuschi, M., Smiraglia, C., Diolaiuti, G. A., 2018. Combination of UAV and terrestrial photogrammetry to assess rapid glacier evolution and map glacier hazards. *Natural Hazards and Earth System Sciences*, 18(4), 1055–1071. https://nhess.copernicus.org/articles/18/1055/2018/.

Gabrlik, P., la Cour-Harbo, A., Kalvodova, P., Zalud, L., Janata, P., 2018. Calibration and accuracy assessment in a direct georeferencing system for UAS photogrammetry. *International Journal of Remote Sensing*, 39(15-16), 4931-4959. https://doi.org/10.1080/01431161.2018.1434331.

Immerzeel, W., Kraaijenbrink, P., Shea, J., Shrestha, A., Pellicciotti, F., Bierkens, M., de Jong, S., 2014. High-resolution monitoring of Himalayan glacier dynamics using unmanned aerial vehicles. *Remote Sensing of Environment*, 150, 93-103. https://www.sciencedirect.com/science/article/pii/S003442571400176X.

Leica Infinity Development Team, 2022. Leica Infinity Software. https://leica-geosystems.com/products/gnss-systems/software/leica-infinity.

Maier, K., Nascetti, A., van Pelt, W., Rosqvist, G., 2022. Direct photogrammetry with multispectral imagery for UAV-based snow depth estimation. *ISPRS Journal of Photogrammetry and Remote Sensing*, 186, 1-18. https://www.sciencedirect.com/science/article/pii/S0924271622000296.

Paul, F., Rastner, P., Azzoni, R. S., Diolaiuti, G., Fugazza, D., Le Bris, R., Nemec, J., Rabatel, A., Ramusovic, M., Schwaizer, G., Smiraglia, C., 2020. Glacier shrinkage in the Alps continues unabated as revealed by a new glacier inventory from Sentinel-2. *Earth System Science Data*, 12(3), 1805–1821. https://essd.copernicus.org/articles/12/1805/2020/.

Rabah, M., Basiouny, M., Ghanem, E., Elhadary, A., 2018. Using RTK and VRS in direct geo-referencing of the UAV imagery. *NRIAG Journal of Astronomy and Geophysics*, 7(2), 220-226. https://www.sciencedirect.com/science/article/pii/S2090997718300257.

Scaioni, M., Corti, M., Diolaiuti, G., Fugazza, D., Cernuschi, M., 2017. LOCAL AND GENERAL MONITORING OF FORNI GLACIER (ITALIAN ALPS) USING MULTI-PLATFORM STRUCTURE-FROM-MOTION PHOTOGRAMMETRY. *The International Archives of the Photogrammetry, Remote Sensing and Spatial Information Sciences*, XLII-2/W7, 1547–1554. https://www.int-arch-photogramm-remote-sens-spatial-inf-sci.net/XLII-2-W7/1547/2017/.

Scaioni, M., Crippa, J., Corti, M., Barazzetti, L., Fugazza, D., Azzoni, R., Cernuschi, M., Diolaiuti, G. A., 2018. TECHNICAL ASPECTS RELATED TO THE APPLICATION OF SFM PHOTOGRAMMETRY IN HIGH MOUNTAIN. *The International Archives of the Photogrammetry, Remote Sensing and Spatial Information Sciences*, XLII-2, 1029–1036. https://www.int-arch-photogramm-remote-sens-spatial-inf-sci.net/XLII-2/1029/2018/.

Taddia, Y., Stecchi, F., Pellegrinelli, A., 2020. Coastal Mapping Using DJI Phantom 4 RTK in Post-Processing Kinematic Mode. *Drones*, 4(2). https://www.mdpi.com/2504-446X/4/2/9.

Tonolo, G., F., Cina, A., Manzino, A., Fronteddu, M., 2020. 3D GLACIER MAPPING BY MEANS OF SATELLITE STEREO IMAGES: THE BELVEDERE GLACIER CASE STUDY IN THE ITALIAN ALPS. *The International Archives of the Photogrammetry, Remote Sensing and Spatial Information Sciences*, XLIII-B2-2020, 1073–1079. https://www.int-arch-photogramm-remote-sens-spatial-inf-sci.net/XLIII-B2-2020/1073/2020/.

Turner, D., Lucieer, A., Wallace, L., 2014. Direct Georeferencing of Ultrahigh-Resolution UAV Imagery. *IEEE Transactions on Geoscience and Remote Sensing*, 52(5), 2738-2745.

Westoby, M., Brasington, J., Glasser, N., Hambrey, M., Reynolds, J., 2012. 'Structure-from-Motion' photogrammetry: A low-cost, effective tool for geoscience applications. *Geomorphology*, 179, 300-314. https://www.sciencedirect.com/science/article/pii/S0169555X12004217.